Available online at www.sciencedirect.com

ScienceDirect

Energy Procedia 92 (2016) 880 – 885

Energy Procedia

6th International Conference on Silicon Photovoltaics, SiliconPV 2016

Characterization of Cu and Ni precipitates in n- and p-type Czochralski-grown silicon by photoluminescence

Chang Sun[a,*], Hieu T. Nguyen[a], Fiacre E. Rougieux[a], Daniel Macdonald[a]

[a] *Research School of Engineering, College of Engineering and Computer Science, The Australian National University, Canberra, ACT 2601, Australia*

Abstract

Photoluminescence (PL) images and micro-PL maps were taken on n- and p-type, Cu- and Ni-doped monocrystalline silicon wafers, in which the Ni and Cu had precipitated during ingot growth. Markedly different distributions of the precipitates were observed in the n- and p-type samples: in the n-type Cu-doped samples, a particle-lean ring structure was observed, dividing the sample into a central region and an edge region. Particles were distributed randomly in both regions, and those in the edge region had lower contrast, smaller sizes and higher densities than those in the central region. In the p-type Cu-doped samples, by contrast, the precipitates occurred in lines along <110> orientations. The Ni-doped samples showed similar features to the Cu samples. The different precipitation behaviours in n- and p-type samples are conjectured to be related to different concentrations of interstitials and vacancies in n- and p-type silicon.

Peer review by the scientific conference committee of SiliconPV 2016 under responsibility of PSE AG.

Keywords: Si; Ni and Cu precipitates; photoluminescence; intersitials and vacancies

1. Introduction

Cu and Ni are two common metallic impurities in Si.[1-3] Due to their high diffusivities and solubilities, contamination happens easily during the production and processing of wafers. [2, 3] Cu and Ni primarily exist as precipitates in silicon at room temperature.[1, 2] The precipitates introduce deep band-like states in the bandgap of silicon and thus can degrade the carrier lifetimes significantly.[1-5] As a result, the recombination-active areas due

* Corresponding author.
E-mail address: chang.sun@anu.edu.au

Peer review by the scientific conference committee of SiliconPV 2016 under responsibility of PSE AG.
doi:10.1016/j.egypro.2016.07.097

to the precipitates are visible in PL images. In this work we use both PL imaging and micro-PL mapping to characterize the precipitates in Czochralski-grown (Cz) silicon, and compare the precipitates in n- and p-type silicon.

2. Experiments

The samples used in this study were cut from six Cz ingots grown by SiliConsutlant [6]. For each type, one ingot was grown as a control ingot, one was intentionally doped with Cu and one doped with Ni. The boron and phosphorus doping levels of the samples were within the $(1.2\pm0.2)\times10^{16}$ cm^{-3} range. The Ni concentrations were about 1.1×10^{14} cm^{-3}, and the Cu concentrations were 2.2×10^{15} cm^{-3} in both n- and p-type samples, estimated by applying Scheil's equation to the concentration added to the melt, and the effective segregation coefficients[7]. The wafers were silicon-etched and then passivated with Plasma-Enhanced Chemical Vapor Deposited (PECVD) SiN films. The PL images were obtained using a LIS-R1 PL imaging system from BT imaging. The pixel size of the PL images was about 23 μm. The micro-PL mapping system used in this study was a Horiba T64000 equipped with a confocal microscope. For this study the wavelength of the incident laser beam was 810±10nm, and on-sample average intensity was 11~12 mW. The illuminated spot size was 3.5 μm in diameter, and the scanning step size was 10μm in both *x* and *y* directions. The micro-PL maps allowed more highly resolved inspection of the precipitates, due partly to the smaller pixel size, but also due to the higher injection level, which reduced lateral carrier diffusion during the measurement.[8, 9] All measurements were performed at room temperature.

3. Results and discussion

3.1. PL images

Figure 1 shows the PL count rate images of the samples. The images of the control samples (1(a) and 1(b)) show relatively uniform high-signal areas. In the image of the n-type Cu-doped sample (1(c)), the particles are not visible. A bright ring-structure can be seen, dividing the sample into a central and an edge region. In the image of the n-type Ni-doped sample (1(e)), the particles are visible and are randomly distributed, and a central region and an edge region can be seen. In the p-type Cu-doped and Ni-doped samples (1(d) and 1(f)), the horizontal and upright straight dark lines are laser labels. Ignoring these labels, the lined-up colonies of particles in two perpendicular orientations can be seen. The orientations were identified as the <110> direction by cleaving the samples.

3.2. Micro-PL images

We then mapped several areas on all samples using the micro-PL system. The mapped areas on the samples are indicated in Figure 1 as red squares or rectangles. Almost no particles were seen in the micro-PL images of the control samples, as shown by Figure 2. The particles are visible in the images of the n-type Cu-doped sample (Figures 3 and 4). Comparing Figure 3(a) and (b), the particles in the edge region have lower contrast, smaller sizes and higher densities than those in the central region. A much lower density of particles is observed in the ring region (Figure 4). In the p-type Cu-doped sample image (Figure 5), similar features with the PL image are observed. For each type, the images of the Ni-doped sample (Figures 6 and 7) show similar features with the Cu-doped sample.

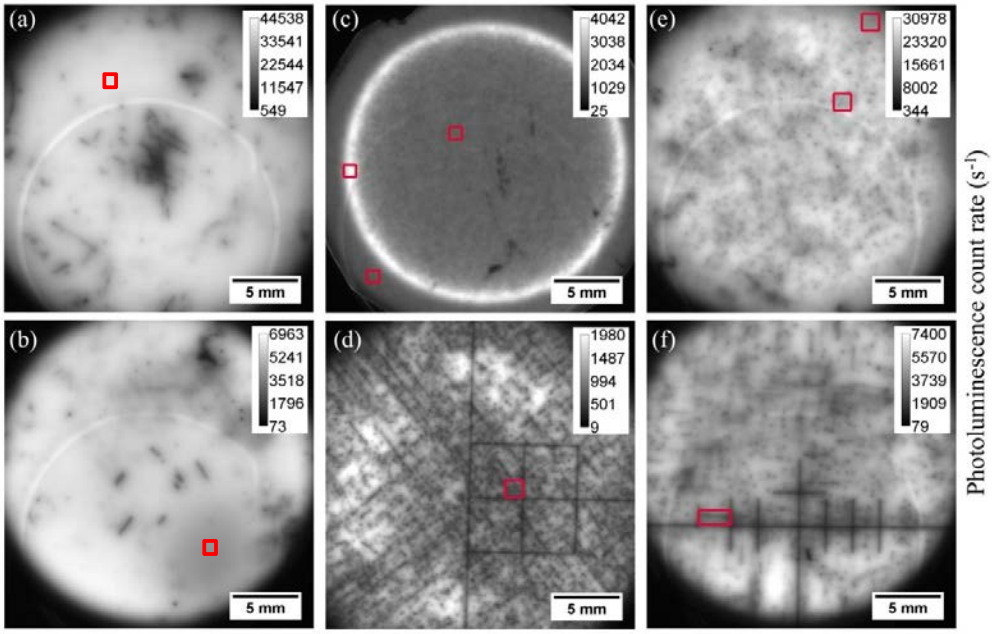

Fig. 1. PL images of the (a) n-type control, (b) p-type control, (c) n-type Cu-doped, (d) p-type Cu-doped, (e) n-type Ni-doped and (f) p-type Ni-doped samples. The red labels illustrate the areas where the micro-PL images are taken.

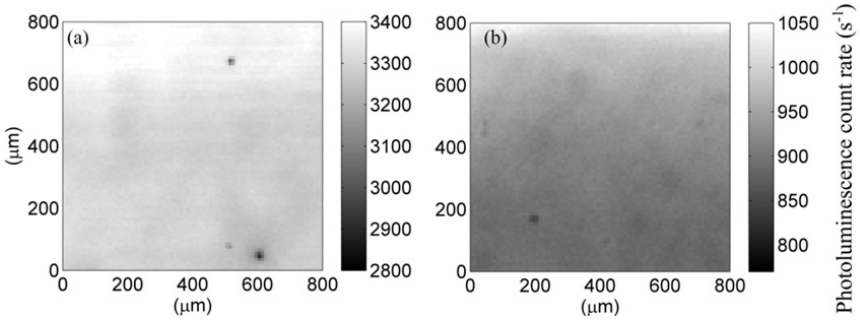

Fig. 2. Micro-PL images of two 800μm×800μm areas on the (a) n-type and (b) p-type control sample.

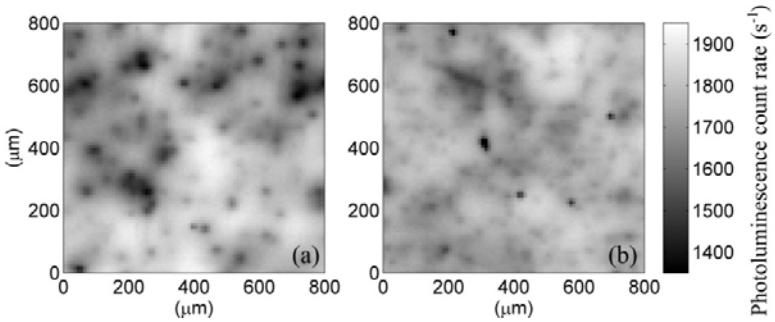

Fig. 3. Micro-PL images of two 800μm×800μm areas on the n-type Cu-doped sample in the (a) central region and (b) edge region.

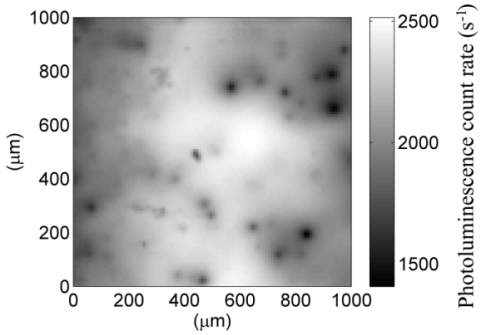

Fig. 4. Micro-PL images of a 1mm×1mm area on the n-type Cu-doped sample in the ring region.

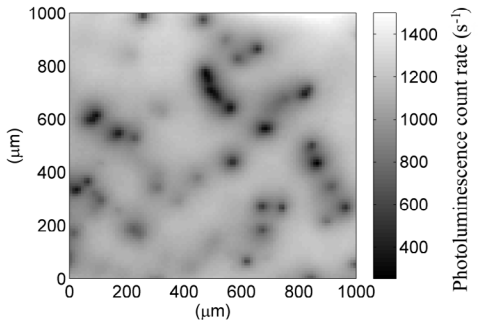

Fig. 5. Micro-PL image of a 1mm×1mm area on the p-type Cu-doped sample.

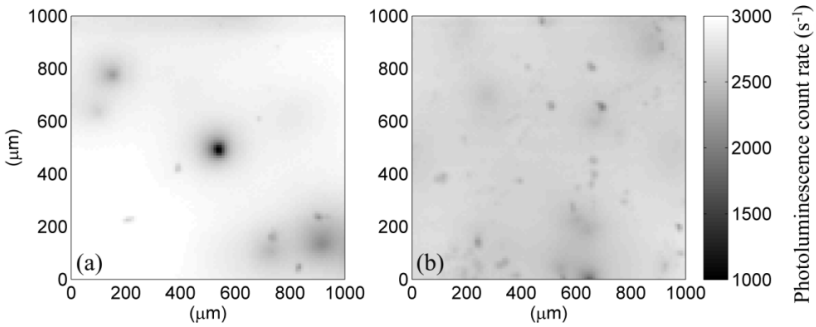

Fig. 6. Micro-PL images of two 1mm×1mm areas on the n-type Ni-doped sample in the (a) central region and (b) edge region.

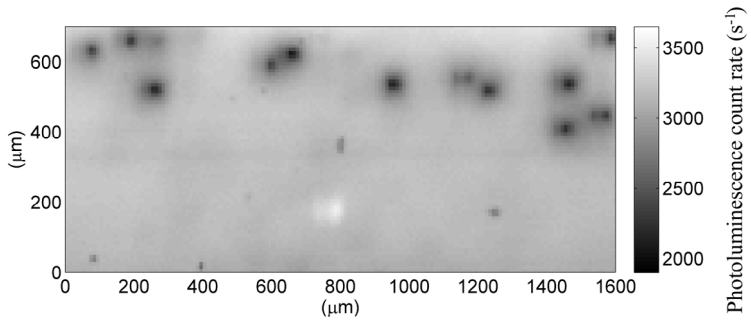

Fig. 7. Micro-PL images of a 1.6mm×0.7mm area on the p-type Ni-doped sample.

3.3. Discussion

Table 1 lists the solubility and diffusivity data of Cu and Ni at 500 °C~700 °C. In the samples in this study, [Ni]= 1.1×10^{14} cm^{-3}, and [Cu]= 2.2×10^{15} cm^{-3}. At 500 °C~600 °C, the solubility is already one order of magnitude lower than the concentration for both Cu and Ni, yet the metals are very mobile at this temperature range. As a result, Cu and Ni should have precipitated quantitatively above 500°C, at which temperature the silicon was intrinsic. Thus the strikingly different precipitation behaviours in n- and p-type samples cannot be explained by the Fermi level effect model, in which precipitates are positively charged in p-type silicon (negatively charged in n-type silicon) leading to a Coulomb repulsion (no coulomb repulsion in n-type) between Cu_i^+ atoms and Cu precipitates.[10]

Table 1. The solubilities and diffusivities of Ni and Cu at 500 °C~700 °C based on Ref.[2]

T /°C	Ni		Cu	
	S (cm^{-3})	D (cm^2/s)	S (cm^{-3})	D (Cu_i^+) (cm^2/s)
500	1.36×10^{13}	1.72×10^{-6}	1.06×10^{14}	1.29×10^{-5}
600	2.45×10^{14}	3.87×10^{-6}	1.38×10^{15}	2.52×10^{-5}
700	2.44×10^{15}	7.35×10^{-6}	1.06×10^{16}	4.30×10^{-5}

The different precipitation behaviours in n- and p-type samples are conjectured to be related to different concentrations of self-interstitials and vacancies in n- and p-type silicon.[11-13] In vacancy-rich region, Cu precipitates distributes more homogeneously and randomly, and there could be circular structures.[11] Our results agree well with those reported in literature, as shown by Figures 3 and 4. In interstitial-rich region, dislocation-related colonies of Cu precipitates were reported in literature.[12] Similar mechanisms should also apply to Ni.[5, 14] The different concentrations of interstitials and vacancies in n- and p-type silicon can be caused by their interactions with the dopant atoms by various mechanisms.[15-18]

4. Conclusion

Both PL imaging and micro-PL mapping were applied to the characterization of Cu and Ni precipitates in n- and p-type Cz silicon. Strikingly different precipitation patterns were observed in n- and p-type samples. For each type, Cu- and Ni-doped samples showed similar features. In n-Si, random and homogeneous distribution of particles in several regions was observed; while in p-Si, the lined-up colonies of particles in two perpendicular orientations were observed. Such a difference in n- and p-type samples is conjectured to be related to different concentrations of self-interstitials and vacancies. A more detailed analysis of the precipitation mechanisms of Ni and Cu in these samples is in progress and will be presented elsewhere.

Acknowledgements

This work has been supported through the Australian Renewable Energy Agency (ARENA), projects 1-GER010 and RND009, and the Australian Centre for Advanced Photovoltaics. Support from the Australian Research Council (ARC) DECRA and Future Fellowships programs are also acknowledged. The authors are in debt to Prof. H. Tan for providing access to the spectroscopic equipment.

References

[1] A. Istratov and E. Weber, “Electrical properties and recombination activity of copper, nickel and cobalt in silicon,” Applied Physics A, vol. 66, (no. 2), pp. 123-136, 1998.
[2] K. Graff, Metal impurities in silicon-device fabrication: Springer Berlin, 2000.
[3] E.R. Weber, “Transition metals in silicon,” Applied Physics A, vol. 30, (no. 1), pp. 1-22, 1983.
[4] M. Seibt, M. Griess, A. Istratov, H. Hedemann, A. Sattler, and W. Schröter, “Formation and properties of copper silicide precipitates in silicon,” physica status solidi (a), vol. 166, (no. 1), pp. 171-182, 1998.
[5] M. Seibt, H. Hedemann, A. Istratov, F. Riedel, A. Sattler, and W. Schröter, “Structural and electrical properties of metal silicide precipitates in silicon,” physica status solidi(a), vol. 171, (no. 1), pp. 301-310, 1999.
[6] http://www.siliconsultant.com/.
[7] J.R. Davis Jr, A. Rohatgi, R. Hopkins, P. Blais, P. Rai-Choudhury, J. McCormick, and H. Mollenkopf, “Impurities in silicon solar cells,” Electron Devices, IEEE Transactions on, vol. 27, (no. 4), pp. 677-687, 1980.
[8] P. Gundel, M.C. Schubert, W. Kwapil, J. Schön, M. Reiche, H. Savin, M. Yli‐Koski, J.A. Sans, G. Martinez‐Criado, and W. Seifert, “Micro‐photoluminescence spectroscopy on metal precipitates in silicon,” physica status solidi (RRL)-Rapid Research Letters, vol. 3, (no. 7‐8), pp. 230-232, 2009.
[9] P. Gundel, F.D. Heinz, M.C. Schubert, J.A. Giesecke, and W. Warta, “Quantitative carrier lifetime measurement with micron resolution,” J. Appl. Phys., vol. 108, (no. 3), pp. 033705, 2010.
[10] R. Sachdeva, A. Istratov, and E. Weber, “Recombination activity of copper in silicon,” Appl. Phys. Lett., vol. 79, (no. 18), pp. 2937-2939, 2001.
[11] Z. Xi, J. Chen, D. Yang, A. Lawerenz, and H. Moeller, “Copper precipitation in large-diameter Czochralski silicon,” J. Appl. Phys., vol. 97, (no. 9), pp. 094909, 2005.
[12] W. Wang, D. Yang, X. Ma, and D. Que, “Effect of silicon interstitials on Cu precipitation in n-type Czochralski silicon,” J. Appl. Phys., vol. 103, (no. 9), pp. 3534, 2008.
[13] Z. Xi, D. Yang, J. Chen, J. Xu, Y. Ji, D. Que, and H. Moeller, “Influence of copper precipitation on oxygen precipitation in Czochralski silicon,” Semicond. Sci. Technol., vol. 19, (no. 3), pp. 299, 2004.
[14] Z. Xi, D. Yang, J. Chen, D. Que, and H. Moeller, “Nickel precipitation in large-diameter Czochralski silicon,” Physica B: Condensed Matter, vol. 344, (no. 1), pp. 407-412, 2004.
[15] A. De Kock and W. Van de Wijgert, “The effect of doping on the formation of swirl defects in dislocation-free czochralski-grown silicon crystals,” J. Cryst. Growth, vol. 49, (no. 4), pp. 718-734, 1980.
[16] E. Dornberger, D. Gräf, M. Suhren, U. Lambert, P. Wagner, F. Dupret, and W. von Ammon, “Influence of boron concentration on the oxidation-induced stacking fault ring in Czochralski silicon crystals,” J. Cryst. Growth, vol. 180, (no. 3), pp. 343-352, 1997.
[17] V. Voronkov and R. Falster, “Dopant effect on point defect incorporation into growing silicon crystal,” J. Appl. Phys., vol. 87, pp. 4126-4129, 2000.
[18] V. Voronkov and R. Falster, “Effect of doping on point defect incorporation during silicon growth,” Microelectron. Eng., vol. 56, (no. 1), pp. 165-168, 2001.